Hypoxia-induced miR-210 contributes to apoptosis of mouse spermatocyte GC-2 cells by targeting Kruppel-like factor 7

JIN-XING LV[1], JIAN ZHOU[1], RUI-QING TONG[1], BIN WANG[2], XUE-LEI CHEN[2], YAN-YAN ZHUANG[1], FEI XIA[1] and XUE-DONG WEI[2]

[1]Reproductive Medicine Center and [2]Department of Urology, The First Affiliated Hospital of Soochow University, Suzhou, Jiangsu 215006, P.R. China

Received January 12, 2018; Accepted September 14, 2018

DOI: 10.3892/mmr.2018.9644

Abstract. The aim of the present study was to investigate the underlying mechanisms of hypoxia-induced microRNA (miR)-210 effects on mouse GC-2spd (GC-2) cells. GC-2 cells were subjected to hypoxia or normoxia for 12, 24, 48 and 72 h. Apoptosis of GC-2 cells was detected using terminal deoxynucleotidyl-transferase-meditated dUTP nick end labeling and flow cytometry. Reverse transcription-quantitative polymerase chain reaction was performed to analyze the expression of miR-210. Hypoxia-inducible factor-1α (HIF-1α), caspase-3, B-cell lymphoma 2, apoptosis regulator BAX and Kruppel-like factor 7 (KLF7) protein expression levels were detected by western blotting. Luciferase reporter gene assays were used to assess the targeting effects of miR-210 on KLF7. Hypoxia induced GC-2 cell apoptosis and increased the expression of HIF-1α and pro-apoptotic proteins; however, decreased anti-apoptotic protein expression levels. Furthermore, hypoxia resulted in the upregulation of miR-210 in GC-2 cells. HIF-1α and miR-210 were involved in the apoptosis of GC-2 cells by mediating the expression of apoptosis-associated proteins. Furthermore, KLF7 was directly targeted by miR-210 to influence the apoptosis of GC-2 cells subjected to hypoxia. The results suggested that hypoxia-induced miR-210 stimulated the activation of the apoptosis signaling pathway and contributed to the apoptosis of GC-2 cells by targeting KLF7.

Introduction

Infertility, a worldwide reproductive health problem, affects 10-15% of couples (1). In particular, more than one-half of the cases are due to male infertility, and 60-75% male infertility cases are idiopathic, which is frequently the most difficult form of infertility to treat (2). Male infertility may result from a number of factors, including azoospermia, oligospermia, asthenospermia, orchitis and varicoceles (3). The pathogenesis of male infertility is usually derived from genetic and environmental factors. In terms of environmental factors, previous studies suggested that chronic hypoxia induces male infertility (4,5). A number of previous studies further suggested that hypoxia may induce the apoptosis of spermatogenic cells and spermatogenesis in mice and hypoxia-induced rat models of male infertility (6-8). However, the underlying molecular mechanisms of this effect remain to be elucidated.

MicroRNAs (miRNAs), a family of small non-coding RNAs (~22 nt), serve an important role in mediating post-transcriptional gene silencing by sequence-selective targeting of mRNAs (9). It was demonstrated that miRNAs are important regulators of cell growth, differentiation, apoptosis, metabolism and tumorigenesis (10). Previously, numerous miRNAs have been identified to be exclusively or preferentially expressed in mice testes, suggesting the important role of miRNAs in translational repression during spermatogenesis (11,12). Previous studies demonstrated that certain miRNAs may be regulated by hypoxia (6,13), and miRNA (miR)-210 is the most induced miRNA under hypoxia of all the hypoxia-induced miRNAs (14).

miR-210 targets, including E2F transcription factor 3, autophagy-related protein 7, iron-sulfur cluster scaffold protein and Kruppel-like factor 7 (KLF7), have effects on cell proliferation, autophagy, adenosine triphosphate metabolism and angiogenesis (15-19). Among the miR-210 targets, KLF7 is a member of the Kruppel-like factors (KLFs) family and, due to its wide expression in a number of adult human tissues, is additionally termed ubiquitous KLF (20). In the KLFs family, 17 members (KLF1-KLF17) have been identified in mammals, exerting effects on cell proliferation, differentiation and apoptosis (21). It was additionally demonstrated that chicken KLF7 inhibits preadipocyte differentiation and promotes preadipocyte proliferation (22). However, the function of KLF7 in hypoxia-induced apoptosis of GC-2spd (GC-2) cells has not been fully elucidated. The present study investigated whether and how miR-210 contributes to the apoptosis of spermatocytes by targeting KLF7.

Correspondence to: Dr Xue-Dong Wei, Department of Urology, The First Affiliated Hospital of Soochow University, 188 Shizi Street, Suzhou, Jiangsu 215006, P.R. China
E-mail: xuedong_wei@sina.cn

Key words: hypoxia, microRNA-210, Kruppel-like factor 7, apoptosis, mouse spermatocyte GC-2 cells

Materials and methods

Cell treatment and transfection. GC-2 cells (a mouse pachytene spermatocyte-derived immortalized cell line) were obtained from the American Type Culture Collection (Manassas, VA, USA) and cultured in RPMI 1640 medium (Invitrogen; Thermo Fisher Scientific, Inc., Waltham, MA, USA) supplemented with 10% fetal bovine serum (Gibco; Thermo Fisher Scientific, Inc.) and antibiotics (100 U/ml penicillin and 100 U/ml streptomycin). The cells were subsequently subjected to hypoxia (1% O_2, 5% CO_2, 10% H_2 and 85% N_2) at 37˚C in a hypoxia workstation (Invivo$_2$; The Baker Company, Inc., Sanford, ME, USA) for 12, 24, 48 or 72 h or incubated in normoxia (21% O_2 and 5% CO_2) as a control. RNA and protein isolation, terminal deoxynucleotidyl-transferase-meditated dUTP nick end labeling (TUNEL) staining and flow cytometry analysis were performed on the GC-2 cells at all the indicated time points.

GC-2 cells were cultured until they reached 80% confluence in six-well dishes, washed once with PBS and subsequently transfected with small interfering (si)RNA with sequences as follows: sense, 5'-GGGCCAUAUUCAUGUCUAUUU-3' and antisense, 5'-AUAGACAUGAAUAUGGCCCUU-3' for mouse hypoxia-inducible factor-1α (HIF-1α); sense, 5'-UUC UCCGAACGUGUCACGUTT-3' and antisense, 5'-ACGUGA CACGUUCGGAGAATT-3' as a negative control (NC; all purchased from Guangzhou RiboBio Co., Ltd., Guangzhou, China). siRNA was transfected at a final concentration of 100 nM. In addition, full-length KLF7 cDNA fragments (20 ng; Guangzhou RiboBio Co., Ltd.) were cloned into the pcDNA3.1-Myc-His vector between the *Kpn*1 and *Not*1 restriction sites (Invitrogen; Thermo Fisher Scientific, Inc.), generating pcDNA3.1-KLF7. The empty pcDNA3.1 vector was used as the control. The GC2 cells were cultured in the hypoxia workstation for 48 h or were transfected with miR-210 mimics (0.4 nM) or inhibitors (0.4 nM), as well as pcDNA3.1-KLF7 (50 nM) using Lipofectamine® 2000 (Invitrogen; Thermo Fisher Scientific, Inc.), according to the manufacturer's protocol. The sequence of the miRNA-210 mimic was: 5'-CUGUGCGUGUGACAGCGGCUGA-3'. The sequence of the NC miRNA mimic was: 5'-UUCUCCGAACGUGUC ACGU-3'. The sequence of the anti-miR-210 inhibitor was: 5'-UCAGCCGCUGUCACACGCACAG-3'. The sequence of the NC inhibitor was: 5'-CAGUACUUUUGUGUAGUACAA-3'. Subsequently, the cells were cultured in the hypoxia workstation for 12, 24, 48 and 72 h. Experiments were routinely performed in triplicate wells and repeated three times. *TUNEL assay*. TUNEL assays were performed to detect the apoptosis of GC-2 cells using TUNEL fluorescent kit (Wuhan Boster Biological Technology, Ltd., Wuhan, China) according to the manufacturer's protocol. Cells, subjected to hypoxia or normoxia, and then fixed using 4% paraformaldehyde for 1 h at 15-25˚C. Cells were then permeabilized using 0.1% Triton X-100 for 2 min on ice (2-8˚C), followed by fluorescein isothiocyanate (FITC)-labeled TUNEL staining (Roche Diagnostics GmbH, Mannheim, Germany) for 1 h at 37˚C. Following this, cells were counterstained with 1 μg/ml 4',6-diamidino-2-phenylindole (Sigma-Aldrich; Merck KGaA, Darmstadt, Germany) and subsequently mounted in ProLong™ Gold Antifade Mountant (Invitrogen; Thermo Fisher Scientific, Inc.). TUNEL-positive cells were imaged under a fluorescence microscope and imaging system (AF6000; Leica Microsystems GmbH, Wetzlar, Germany), and five fields from each image were quantified (the number of green spots).

Apoptosis assays by flow cytometry. Cells (1x10^6 cells/ml) were subjected to hypoxia as above, washed twice with ice-cold PBS, and subsequently stained with an Annexin V-FITC apoptosis detection kit (BD Pharmingen; BD Biosciences, San Jose, CA, USA) according to the manufacturer's protocol. The apoptosis incidence rate was analyzed using a flow cytometer (FACSCalibur; BD Biosciences) within 1 h of staining. Apoptotic cells were counted and presented as a percentage of the total cell count for each sample. The percentage of FITC-positive cells was analyzed using BD CellQuest™ software version 6.0 (BD Biosciences).

Luciferase assay. The putative miR-210-binding site in the 3' untranslated region (UTR) of the KLF7-mRNA was identified using the TargetScan database (www.targetscan.org). To construct a KLF7 3'UTR luciferase reporter plasmid, the KLF7 3'UTR was amplified from mouse genomic DNA. The 3'-UTR of KLF7, containing the predicted wild-type (Wt) or mutated (Mut) binding sites of miR-210 were amplified using mouse genomic DNA via PCR using DreamTaq DNA Polymerase (Thermo Fisher Scientific, Inc.). The primers used were as follows: KLF7-Wt 3'UTR construct primer forward, 5'-GCA GCCAATGTCCGAAGGA-3', and reverse, 5'-GAGGACCCA ATAAACAGG-3'; KLF7-Mut primer forward, 5'-CCTCTG TGTGCATACATGTACACGCACACGTACACACACCCT CTCAC-3', and reverse, 5'-GTGAGAGGGTGTGTGTACGTG TGCGTGTACATGTATGCACACAGAGG-3'. The thermocycling conditions used were as follows: Initial denaturation at 95˚C for 2 min; followed by 40 cycles of denaturation at 95˚C for 30 sec, annealing at 60˚C for 30 sec, extension at 72˚C for 1 min and a final extension at 72˚C for 5 min. The resulting purified polymerase chain reaction (PCR) products were subsequently cloned into the downstream region of the pGL3vector (Promega Corporation, Madison, WI, USA). Mutant constructs with 6-7 mutated residues in the predicted binding site were generated by site-directed mutagenesis. Subsequently, 293T cells (Shanghai Aiyan Biological Technology Co., Ltd., Shanghai, China) were cotransfected with the pGL3 vectors containing the Wt or Mut 3'UTR luciferase reporter of KLF7, a miR-210 mimics or a control using Lipofectamine® 2000, in addition to *Renilla* luciferase (pRL-TK Vector; Promega Corporation) as a transfection efficiency control. After 48 h, the luciferase signal was analyzed using the Dual-Luciferase Reporter Assay kit (Promega Corporation) according to the manufacturer's protocol. The results are presented as the relative luciferase activity (firefly luciferase/*Renilla* luciferase). Each experiment was repeated three times.

RNA isolation and reverse transcription-quantitative (RT-q)PCR. miRNA was extracted from treated GC-2 cells using the miRVana miRNA Isolation kit (Ambion; Thermo Fisher Scientific, Inc.) according to the manufacturer's protocol. cDNA was synthesized from 1 μg total RNA using a miRNA RT kit (Applied Biosystems; Thermo Fisher Scientific, Inc.) at 37˚C for 15 min and 85˚C for 5 sec. The miR-210 Bulge-Loop TMmiR-210-3p RT-qPCR Primer

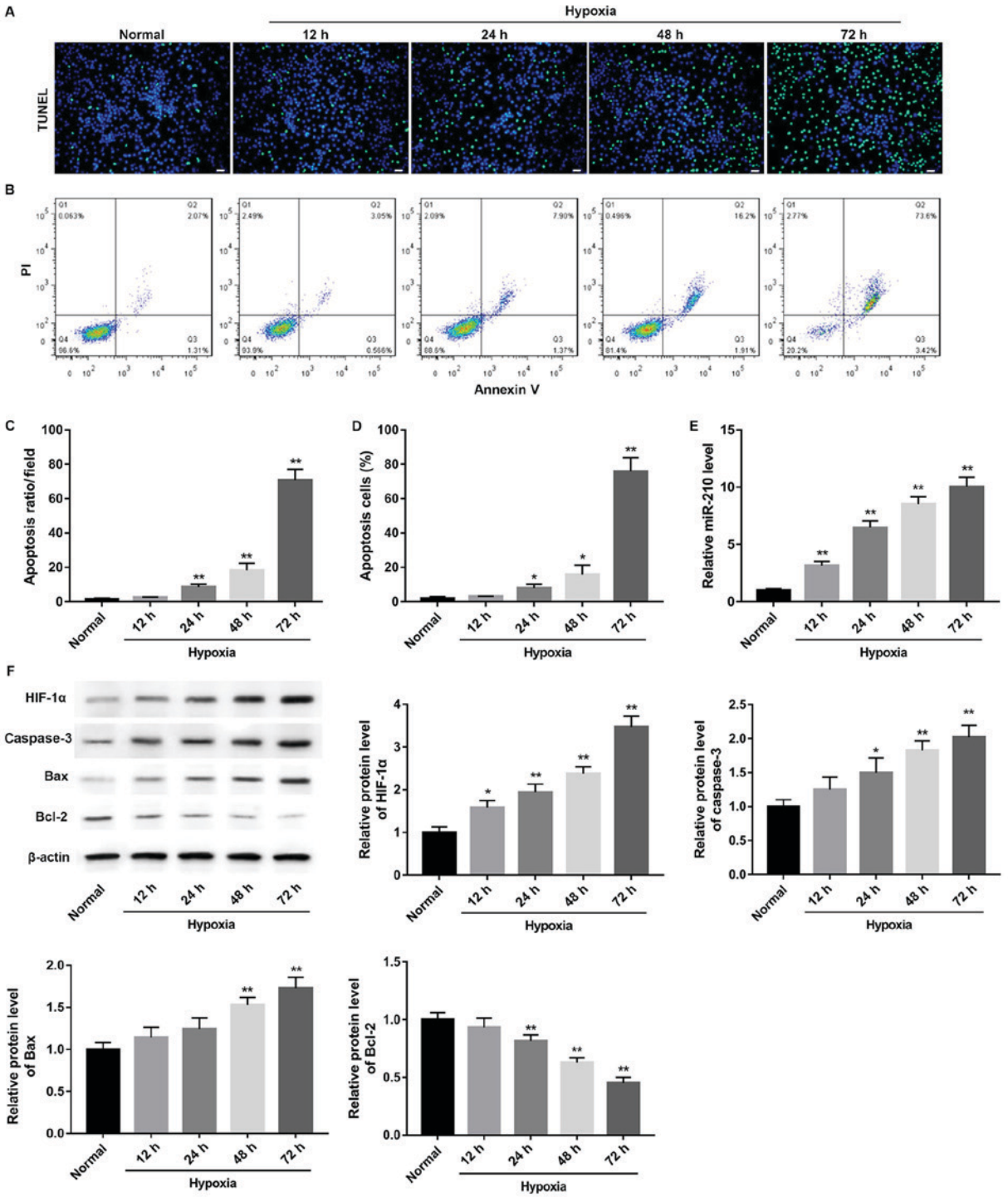

Figure 1. Hypoxia induces apoptosis of GC-2 cells at different time points. (A) TUNEL staining results of GC-2 cells. Scale bar, 20 μm. (B) Representative graphs of flow cytometry analysis. (C) Apoptosis rate of GC-2 cells was evaluated by TUNEL staining. (D) Apoptotic GC-2 cells were measured by flow cytometry. (E) Reverse transcription-quantitative polymerase chain reaction analysis of miR-210 expression in mouse GC-2 cells subjected to hypoxia for 12, 24, 48 and 72 h. (F) Western blot analysis for HIF-1α, caspase-3, Bax and Bcl-2 protein expression in mouse GC-2 cells subjected to hypoxia for 12, 24, 48 and 72 h. *P<0.05, **P<0.01 vs. respective normal. miR, microRNA; HIF-1α, hypoxia-inducible factor-1α; Bax, apoptosis regulator BAX; Bcl-2, B-cell lymphoma 2; TUNEL, terminal deoxynucleotidyl-transferase-meditated dUTP nick end labeling and flow cytometry; PI, propidium iodide; GC-2, GC-2spd.

Set (Guangzhou RiboBio Co., Ltd.) was used: miR-210 forward primer, 5'-CTGTGCGTGT-3' and miR-210 reverse primer, 5'-CATGATCAGCTGGGCCAAGATCAGCCG-3'; U6 forward primer, 5'-CTCGCTTCGGCAGCACA-3' and U6 reverse primer, 5'-AACGCTTCACGAATTTGCGT-3'. The PCR protocol consisted of an initial denaturation step at 95˚C for 10 min, followed by 45 cycles of denaturation at 95˚C for 10 sec and primer annealing/extension at 60˚C for 60 sec. qPCR was performed using 1 μg cDNA and SYBR-Green (Bio-Rad Laboratories, Inc., Hercules, CA, USA) in a LightCycler rapid thermal cycler system (Roche Applied Science, Penzberg, Germany). The data were standardized to U6. Relative quantification of the target gene was conducted using the comparative Cq ($2^{-\Delta\Delta Cq}$) method (23).

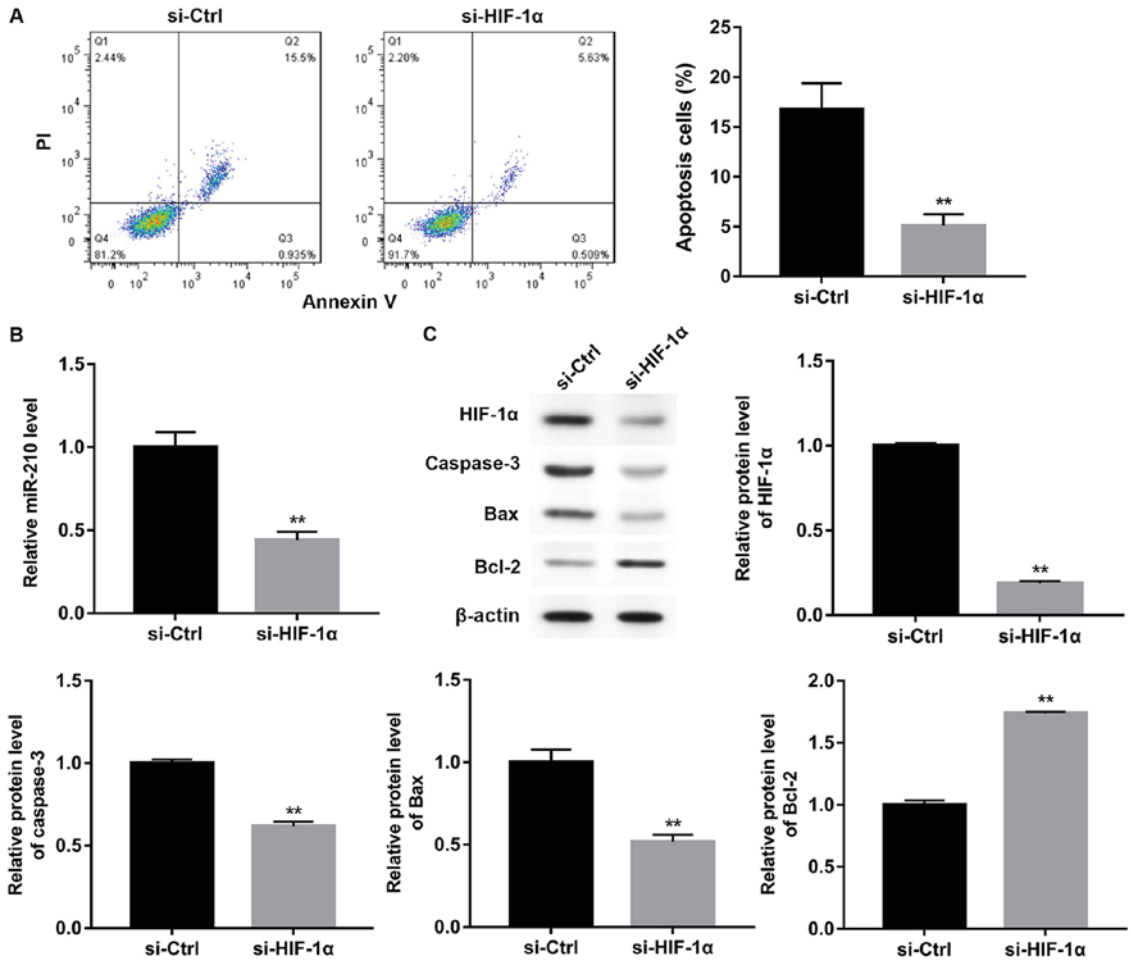

Figure 2. HIF-1α deficiency decreases apoptosis and the expression levels of apoptosis-associated proteins in GC-2 cells. HIF-1α-deficient GC-2 cells and control cells were subjected to hypoxic conditions for 48 h. (A) Cell apoptosis was detected by flow cytometry analysis. (B) Reverse transcription-quantitative polymerase chain reaction analysis detected miR-210 expression in GC-2 cells. (C) HIF-1α and apoptosis-associated proteins were evaluated by western blot analysis. **P<0.01 vs. respective si-Ctrl. HIF-1α, hypoxia-inducible factor-1α; miR, microRNA; si, small interfering; Ctrl, control; PI, propidium iodide; Bax, apoptosis regulator BAX; Bcl-2, B-cell lymphoma 2; GC-2, GC-2spd.

Western blot analysis. Following treatment, proteins were lysed from GC-2 cells in ice-cold radioimmunoprecipitation assay lysis buffer (Beyotime Institute of Biotechnology, Haimen, China), supplemented with protease inhibitors for 1 h to extract total cell protein. Following this, protein concentrations were determined using a bicinchoninic acid kit (Thermo Fisher Scientific, Inc.). Equivalent amounts of protein (20 μg) were separated using 10% SDS-PAGE and electrotransferred onto a nitrocellulose membrane (Bio-Rad Laboratories, Inc.). The membrane was blocked with 5% non-fat dry milk in TBS containing 0.1% Tween (TBST) for 1 h at room temperature. Membranes were subsequently incubated at 4˚C overnight with rabbit anti-caspase 3 antibody (1:1,000; cat. no. 9664), rabbit anti-apoptosis regulator BAX (Bax) antibody (1:500; cat. no. 14796), rabbit anti-B-cell lymphoma 2 (Bcl-2; antibody (1:1,000; cat. no. 3498; all Cell Signaling Technology, Inc., Danvers, MA, USA), rabbit anti-HIF-1α antibody (1:1,000; cat. no. sc-10790; Santa Cruz Biotechnology, Inc., Dallas, TX, USA), rabbit anti-KLF7 antibody (1:500; cat. no. ab197690; Abcam, Cambridge, UK) or rabbit anti-β-actin antibody (1:5,000; cat. no. SAB5500001; Sigma-Aldrich; Merck KGaA). The membranes were washed with TBST and incubated with goat anti-rabbit horseradish peroxidase-conjugated secondary antibodies (1:5,000; cat. no. P044801-2; Dako; Agilent Technologies, Inc., Santa Clara, CA, USA) at room temperature for 1 h. Immunoblotted bands were visualized using an enhanced chemiluminescence kit (GE Healthcare Life Sciences, Little Chalfont, UK). The ChemiDoc Imaging System (Bio-Rad Laboratories, Inc.) and Quantity One™ 1-D Analysis software version 4.6.7 (Bio-Rad Laboratories, Inc.) were used to scan the blots and analyze the density of the blots.

Statistical analysis. Data are presented as the mean ± standard deviation, and each experiment was repeated at least three times. Statistical analyses were conducted using SPSS software version 19.0 (IBM Corp., Armonk, NY, USA). Statistical significance was evaluated using an unpaired two-tailed Student's t-test or by one-way analysis of variance followed by Dunnett's test or the Least Significant Difference test. P<0.05 was considered to indicate a statistically significant difference.

Results

Hypoxia treatment induces GC-2 cell apoptosis. The effects of different hypoxia time periods on GC-2 cell apoptosis

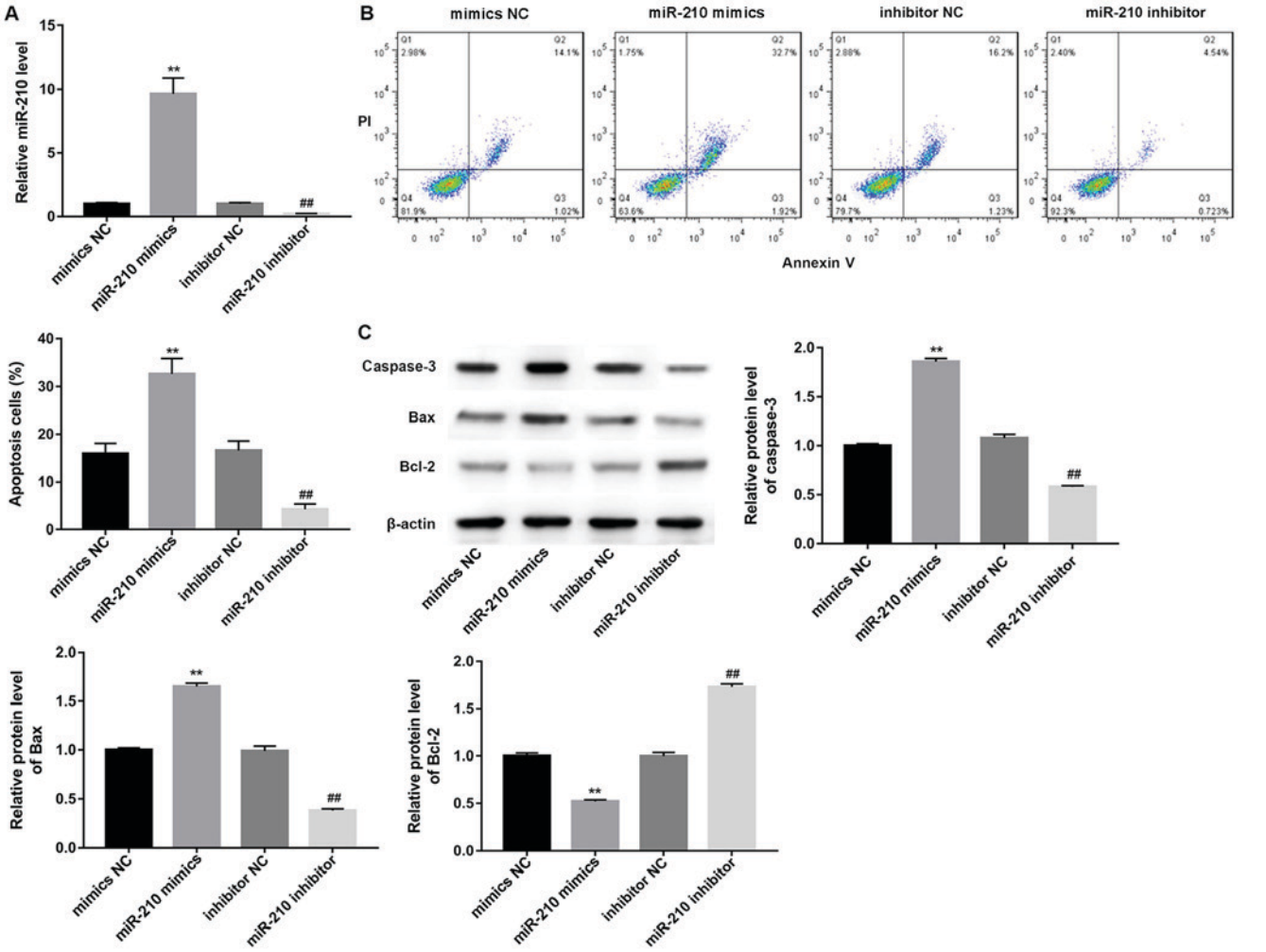

Figure 3. Overexpression of miR-210 induces apoptosis in GC-2 cells. (A) Measurement of transfection efficiency. (B) Analysis of the rate of apoptotic cells transfected with miR-210 mimics, mimics NC, miR-210 inhibitor and inhibitor NC following hypoxic culture. (C) Analysis of apoptosis-associated protein expression in GC-2 cells transfected with miR-210 mimics, mimics NC, miR-210 inhibitor and inhibitor NC. **P<0.01 vs. respective mimics NC; $^{\#\#}$P<0.01 vs. respective inhibitor NC. miR, microRNA; NC, negative control; PI, propidium iodide; Bax, apoptosis regulator BAX; Bcl-2, B-cell lymphoma 2; GC-2, GC-2spd.

were investigated using TUNEL and flow cytometry assays (Fig. 1). The apoptosis at 12, 24, 48 and 72 h of hypoxia are presented in Fig. 1A and C. No difference was observed in the number of apoptotic cells between the hypoxia group at 12 h and the normal group; however, a significant increase in cell apoptosis occurred after 24 h of hypoxia (P<0.01). The results of the flow cytometry assay were consistent with the results of TUNEL staining (Fig. 1B and D). Hypoxia induced a significant increase in the miR-210 expression level compared with the normoxia group (Fig. 1E; P<0.01). Furthermore, the HIF-1α protein expression levels were significantly increased after 12 h of hypoxia (Fig. 1F; P<0.01).

Subsequently, the effect of different time periods of hypoxia on the apoptosis pathway in GC-2 cells was determined by measuring apoptosis-associated protein expression levels at 12, 24, 48 and 72 h following hypoxia. The results demonstrated that the pro-apoptotic proteins caspase-3 and Bax were significantly increased in the hypoxia group compared with the normoxia group in GC-2 cells after 48 h (Fig. 1F; P<0.01). However, the anti-apoptotic protein Bcl-2 was significantly decreased after 24 h of hypoxia (Fig. 1F; P<0.01).

Hypoxia-induced HIF-1α mediates apoptosis of GC-2 cells. A previous study suggested that HIF-1α is involved in mouse spermatocyte apoptosis during hypoxia (6). Therefore, whether HIF-1α silencing affected apoptosis in GC-2 cells and whether the alteration of miR-210 expression was induced by hypoxia was additionally examined. The results demonstrated that the apoptosis of GC-2 cells treated with HIF-1α silencing subjected to hypoxia for 48 h was significantly decreased compared with the null vector group (Fig. 2A; P<0.01). Additionally, interference with HIF-1α-siRNA resulted in a significant decrease in the expression of miR-210 (Fig. 2B; P<0.01), HIF-1α, caspase-3 and Bax, and a significant increase in the expression of Bcl-2 (Fig. 2C; P<0.01).

Upregulation of miR-210 induces apoptosis of GC-2 cells. A previous study suggested that miR-210 is upregulated in the testes of patients with non-obstructive azoospermia (24). In addition, it was demonstrated that miR-210 serves an important role in cell adaptation to hypoxia by regulating a HIF-1-dependent pathway (25). Therefore, it was hypothesized that alteration of miR-210 may affect the apoptosis rate of GC-2 cells under hypoxic conditions. Therefore, the role of miR-210

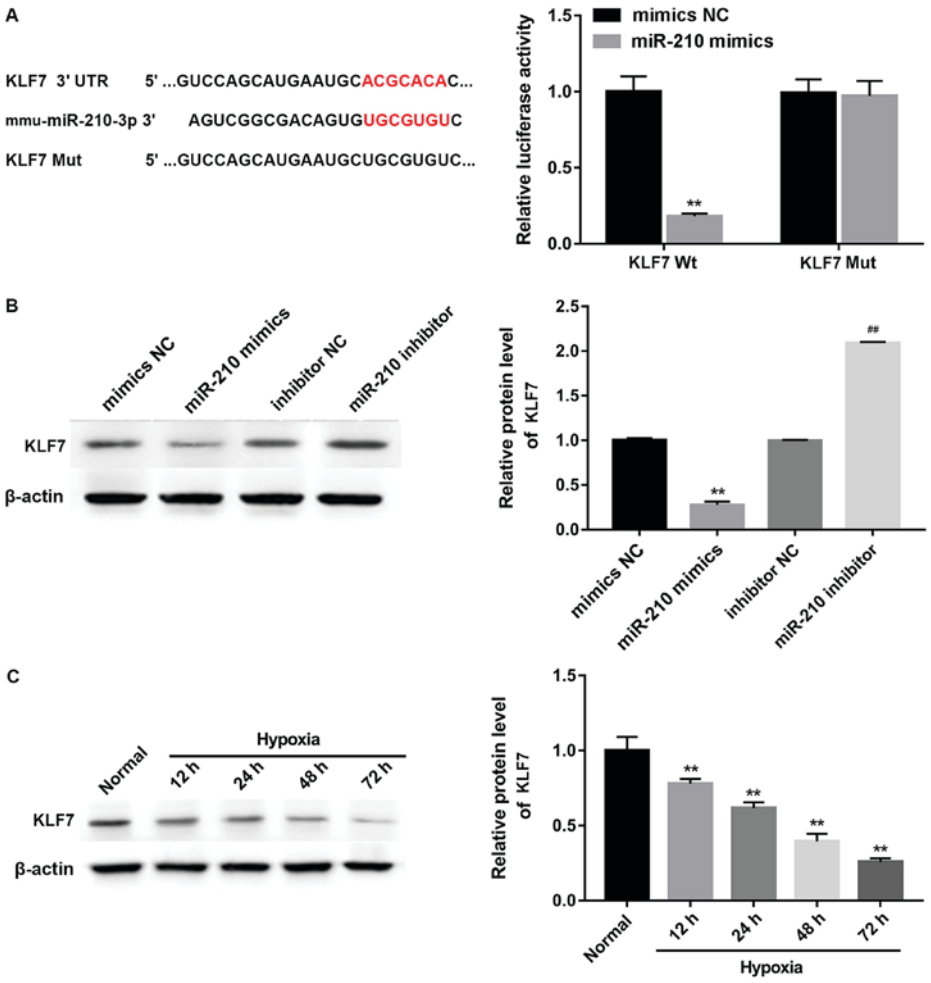

Figure 4. miR-210 target prediction. (A) Interaction between miR-210 and the 3'UTR of KLF7 was predicted using TargetScan (red letters indicate the binding sites), and luciferase activity was assessed by a luciferase assay. **P<0.01 vs. mimics NC. (B) miR-210 effect on KLF7 expression. **P<0.01 vs. mimics NC; ##P<0.01 vs. inhibitor NC. (C) KLF7 protein expression level in GC-2spd cells under hypoxic culture conditions. **P<0.01 vs. normal. miR, microRNA; KLF7, Kruppel-like factor 7; 3'UTR, 3'untranslated region; Wt, wild-type; Mut, mutant; NC, negative control.

in the apoptosis of hypoxia-induced cells was examined. As presented in Fig. 3A, transfection of GC-2 cells with miR-210 mimics or a miR-210 inhibitor had high transfection efficiency. The number of apoptotic GC-2 cells transfected with the miR-210 mimics was significantly increased compared with the mimic NC group under hypoxic conditions (Fig. 3B; P<0.01). Conversely, the apoptosis of GC-2 cells was significantly decreased in the miR-210 inhibitor group (Fig. 3B; P<0.01). Overexpression of miR-210 resulted in a significant increase in the expression of caspase-3 and Bax, and a significant decrease in the expression of Bcl-2 (Fig. 3C; P<0.01). Converse results were observed for the suppression of miR-210 (Fig. 3C), suggesting that miR-210 is involved in the apoptotic pathway of GC-2 cells following hypoxia.

KLF7 is directly targeted by miR-210. As the 3'UTR of the KLF7-mRNA has a putative miR-210-binding site, identified using the TargetScan database (www.targetscan.org), KLF7 was predicted as a potential target of miR-210. To identify whether the KLF7 gene was targeted by miR-210 directly in GC-2 cells, luciferase reporter assays were performed. As presented in Fig. 4A, there was a significant decrease in luciferase activity following cotransfection of GC-2 cells in the KLF7 Wt group with the miR-210 mimics and the luciferase reporter gene (P<0.01); however, the KLF7 Mut demonstrated no difference in luciferase activity between the miR-210 mimics and the mimics NC groups. Overexpression of miR-210 with the mimics significantly decreased the expression of KLF7 (P<0.01); however, treatment with an inhibitor of miR-210 significantly increased KLF7 expression (Fig. 4B; P<0.01). In addition, the expression of KLF7 protein in hypoxic GC-2 cells at each time point was significantly decreased compared with the normal cells (Fig. 4C; P<0.01), suggesting that hypoxia significantly decreased KLF7 protein expression in GC-2 cells.

miR-210 affects apoptosis in GC-2 cells by targeting KLF7. To further determine whether the altered miR-210 and KLF7 expression levels are associated with GC-2 cell apoptosis, the apoptosis of GC-2 cells transfected with the miR-210 mimics and/or KLF7 mimics was assessed by flow cytometry. Under hypoxic conditions, overexpression of miR-210 significantly increased apoptosis, whereas cotransfection of the miR-210 mimics and the KLF7 mimics in GC-2 cells significantly decreased the effects of the miR-210 mimics on cell apoptosis (Fig. 5A; P<0.05). In addition, it was identified that KLF7

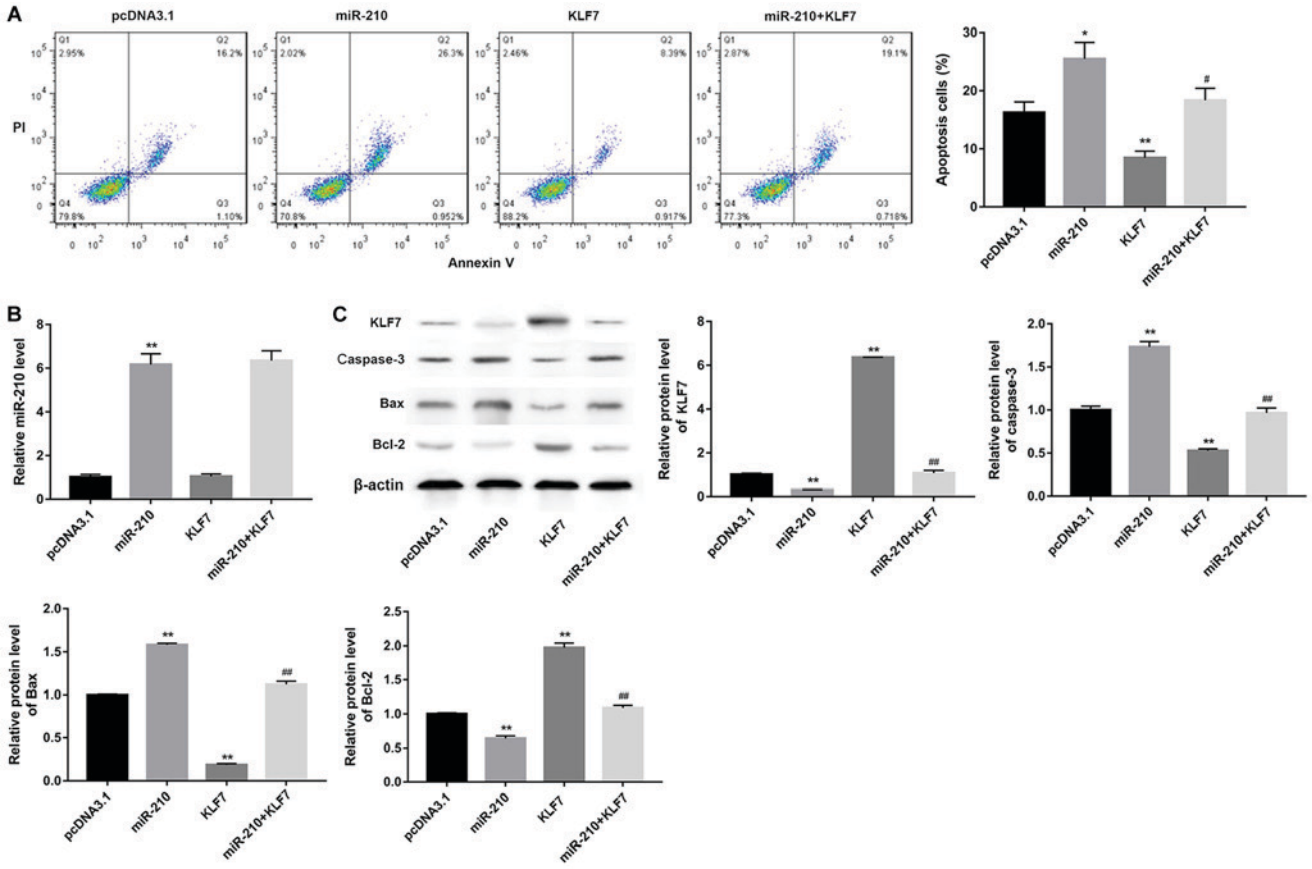

Figure 5. miR-210 promotes apoptosis of GC-2 cell by targeting KLF7. GC-2 cells were transfected with pcDNA3.1, miR-210 mimics, KLF7 mimics and miR-210 mimics + KLF7 mimics following hypoxic for 48 h. (A) Analysis of apoptotic cells. (B) Analysis of miR-210 expression. (C) Analysis of apoptosis-associated protein expression. *P<0.05, **P<0.01 vs. respective pcDNA3.1; $^{\#}$P<0.05, $^{\#\#}$P<0.01 vs. miR-210. miR, microRNA; KLF7, Kruppel-like factor 7; PI, propidium iodide; Bax, apoptosis regulator BAX; Bcl-2, B-cell lymphoma 2; GC-2, GC-2spd.

overexpression had no effect on miR-210 compared with transfection of miR-210 mimics alone (Fig. 5B). The effect of hypoxia-induced miR-210 on apoptosis-associated protein expression was detected by targeting KLF7. The results demonstrated that the protein expression of caspase-3 and Bax was significantly higher in the GC-2 cells transfected with the miR-210 mimics compared with the control cells (Fig. 5C; P<0.01); however, upregulation of KLF7 with the KLF7 mimics cotransfected with miR-210 mimics decreased the effects of the miR-210 mimics on caspase-3 and Bax expression. Converse results were observed for Bcl-2 and KLF7 expression (Fig. 5C).

Discussion

A number of previous studies suggested that hypoxia is a signature of the tumor microenvironment and contributes to proliferation of various types of cancer cells in humans (26-28). However, previous studies on non-cancer cells demonstrated that hypoxia may induce the apoptosis of cardiomyocytes, endothelial cells, astrocytes and muscle cells (29-32). Notably, hypoxia may induce the apoptosis of spermatogenic cells in mice (6). Based on these observations, a hypoxic model of GC-2 cells was established by subjecting cells to hypoxia for different lengths of time. The results of the present study demonstrated that hypoxia induced apoptosis of GC-2 cells and promoted the expression of pro-apoptotic proteins caspase-3 and Bax, while inhibiting the expression of the anti-apoptotic protein Bcl-2 after 48 h of hypoxia. The apoptosis of GC-2 cells additionally increased in a time-dependent manner. These results suggested that the effect of hypoxia on apoptosis-associated protein expression induced apoptosis in GC-2 cells, which may result in the obstruction of spermatogenesis.

HIF-1α serves a key role in the cellular adaptation to hypoxia and ischemia (33). A previous study demonstrated that HIF-1α is involved in the regulation of hypoxia-induced apoptosis (34). Furthermore, it was observed the inhibition of HIF-1α protected cells against apoptosis induced by ischemia and hypoxia (35). Previous studies suggested that miR-210 regulates response to hypoxia in a HIF-dependent way (25,36,37). In the GC-2 cell hypoxia model, it was identified that HIF-1α protein expression levels significantly increased after 12 h of hypoxia. Therefore, considering the effect of hypoxia on GC-2 cell apoptosis and HIF-1α expression, in addition to the association between HIF-1α and miR-210 under hypoxic condition, the present study attempted to determine whether the silencing of HIF-1α affected the apoptosis of GC-2 cells and the alteration of miR-210 expression induced by hypoxia.

The apoptosis of GC-2 cells with HIF-1α silencing demonstrated a significant decrease in apoptosis compared with the null vector group. Additionally, interference of HIF-1α by siRNA resulted in a significant decrease in the miR-210, caspase-3 and Bax expression levels and a significant increase in Bcl-2 expression. In addition, the apoptosis rate of GC-2 cells and the

expression level of pro-apoptotic proteins in the miR-210 mimics group were significantly increased compared with the mimics NC group under hypoxic culture conditions; however, the expression level of anti-apoptotic Bcl-2 was significantly decreased. However, data for depletion of miR-210 were in contrast with the results demonstrating overexpression of miR-210. These results suggested that hypoxia-induced HIF-1α and miR-210 were involved in the apoptotic pathway of GC-2 cells.

KLFs regulate the expression of a number of genes in a variety of cellular processes during embryonic development and in adult cells (38). A previous study on KLF7-null mice suggested that KLF7 is a key factor in the development of the nervous system (39). Previous functional studies demonstrated that KLF7 inhibits preadipocyte differentiation and promotes pre-adipocyte proliferation (22,40). In the present study, the luciferase reporter gene assay demonstrated that KLF7 is a potential target of miR-210. Western blot analysis additionally demonstrated that miR-210 was able to suppress the expression of KLF7. Furthermore, the expression level of KLF7 protein in hypoxic GC-2 cells decreased significantly compared with the control cells at each time point. Under hypoxic conditions, overexpression of miR-210 increased the apoptosis of GC-2 cells and pro-apoptotic protein expression, whereas cotransfection of the miR-210 mimics and the KLF7 mimics decreased the effects of the transfection with miR-210 mimics. Converse effects for Bcl-2 and KLF7 were observed for caspase-3 and Bax. These data suggested that the effects of hypoxia-induced miR-210 expression on apoptosis-associated protein function were via the targeting of KLF7 in GC-2 cells.

In conclusion, the results of the present study suggested that the hypoxia-induced apoptosis of GC-2 cells is mediated by the targeting of KLF7 by miR-210. These results may aid the understanding of the underlying mechanisms of hypoxia-induced GC-2 cell apoptosis, and provide insight for the development of impaired spermatogenesis.

Acknowledgements

Not applicable.

Funding

The present study was supported by grants from the Key Discipline of Medicine of Jiangsu Province (grant no. ZDXKA2016012), the Suzhou Key Medical Center (grant nos. SZXK2015020 and SZZXJ201501), the Suzhou Government (grant nos. LCZX201502 and SYS201754) and the National Natural Science Foundation of China (grant no. 81300537).

Availability of data and materials

The datasets used and/or analyzed during the current study are available from the corresponding author on reasonable request.

Authors' contributions

X-DW and J-XL contributed to the study conception. J-XL, X-DW and FX designed the study. The clinical studies were conducted by JZ and BW, and the experimental studies were conducted by R-QT and X-LC. BW acquired the data and performed the analysis. Y-YZ conducted the statistical analysis. J-XL, JZ and R-QT edited the manuscript. Y-YZ and FX edited the manuscript. All authors read and approved the final manuscript.

Ethics approval and consent to participate

Not applicable.

Patient consent for publication

Not applicable.

Competing interests

The authors declare that they have no competing interests.

References

1. Inhorn MC and Patrizio P: Infertility around the globe: New thinking on gender, reproductive technologies and global movements in the 21st century. Hum Reprod Update 21: 411-426, 2015.
2. Okada H, Tajima A, Shichiri K, Tanaka A, Tanaka K and Inoue I: Genome-wide expression of azoospermia testes demonstrates a specific profile and implicates ART3 in genetic susceptibility. PLoS Genet 4: e26, 2008.
3. Wu H, Sun L, Wen Y, Liu Y, Yu J, Mao F, Wang Y, Tong C, Guo X, Hu Z, *et al*: Major spliceosome defects cause male infertility and are associated with nonobstructive azoospermia in humans. Proc Natl Acad Sci USA 113: 4134-4139, 2016.
4. Verratti V, Berardinelli F, Giulio CD, Bosco G, Cacchio M, Pellicciotta M, Nicolai M, Martinotti S and Tenaglia R: Evidence that chronic hypoxia causes reversible impairment on male fertility. Asian J Androl 10: 602-606, 2008.
5. Torres M, Laguna-Barraza R, Dalmases M, Calle A, Pericuesta E, Montserrat JM, Navajas D, Gutierrez-Adan A and Farré R: Male fertility is reduced by chronic intermittent hypoxia mimicking sleep apnea in mice. Sleep 37: 1757-1765, 2014.
6. Yin J, Bing N, Liao WG and Gao YQ: Hypoxia-induced apoptosis of mouse spermatocytes is mediated by HIF-1α through a death receptor pathway and a mitochondrial pathway. J Cell Physiol 233: 1146-1155, 2018.
7. Reyes JG, Farias JG, Henríquez-Olavarrieta S, Madrid E, Parraga M, Zepeda AB and Moreno RD: The hypoxic testicle: Physiology and pathophysiology. Oxid Med Cell Longev 2012: 929285, 2012.
8. Liao W, Cai M, Chen J, Huang J, Liu F, Jiang C and Gao Y: Hypobaric hypoxia causes deleterious effects on spermatogenesis in rats. Reproduction 139: 1031-1038, 2010.
9. Stark A, Bushati N, Jan CH, Kheradpour P, Hodges E, Brennecke J, Bartel DP, Cohen SM and Kellis M: A single Hox locus in Drosophila produces functional microRNAs from opposite DNA strands. Genes Dev 22: 8-13, 2008.
10. Marignol L, Coffey M, Lawler M and Hollywood D: Hypoxia in prostate cancer: A powerful shield against tumour destruction? Cancer Treat Rev 34: 313-327, 2008.
11. Kotaja N and Sassone-Corsi P: The chromatoid body: A germ-cell-specific RNA-processing centre. Nat Rev Mol Cell Biol 8: 85-90, 2007.
12. Ro S, Park C, Sanders KM, McCarrey JR and Yan W: Cloning and expression profiling of testis-expressed microRNAs. Dev Biol 311: 592-602, 2007.
13. Crosby ME, Devlin CM, Glazer PM, Calin GA and Ivan M: Emerging roles of microRNAs in the molecular responses to hypoxia. Curr Pharm Des 15: 3861-3866, 2009.
14. Huang X, Ding L, Bennewith KL, Tong RT, Welford SM, Ang KK, Story M, Le QT and Giaccia AJ: Hypoxia-inducible mir-210 regulates normoxic gene expression involved in tumor initiation. Mol Cell 35: 856-867, 2009.
15. Giannakakis A, Sandaltzopoulos R, Greshock J, Liang S, Huang J, Hasegawa K, Li C, O'Brien-Jenkins A, Katsaros D, Weber BL, *et al*: miR-210 links hypoxia with cell cycle regulation and is deleted in human epithelial ovarian cancer. Cancer Biol Ther 7: 255-264, 2008.

16. Wang C, Zhang ZZ, Yang W, Ouyang ZH, Xue JB, Li XL, Zhang J, Chen WK, Yan YG and Wang WJ: MiR-210 facilitates ECM degradation by suppressing autophagy via silencing of ATG7 in human degenerated NP cells. Biomed Pharmacother 93: 470-479, 2017.
17. Lee DC, Romero R, Kim JS, Tarca AL, Montenegro D, Pineles BL, Kim E, Lee J, Kim SY, Draghici S, *et al*: miR-210 targets iron-sulfur cluster scaffold homologue in human trophoblast cell lines: Siderosis of interstitial trophoblasts as a novel pathology of preterm preeclampsia and small-for-gestational-age pregnancies. Am J Pathol 179: 590-602, 2011.
18. White K, Lu Y, Annis S, Hale AE, Chau BN, Dahlman JE, Hemann C, Opotowsky AR, Vargas SO, Rosas I, *et al*: Genetic and hypoxic alterations of the microRNA-210-ISCU1/2 axis promote iron-sulfur deficiency and pulmonary hypertension. EMBO Mol Med 7: 695-713, 2015.
19. Gao Y, Cao Q, Lu L, Zhang X, Zhang Z, Dong X, Jia W and Cao Y: Kruppel-like factor family genes are expressed during Xenopus embryogenesis and involved in germ layer formation and body axis patterning. Dev Dyn 244: 1328-1346, 2015.
20. Matsumoto N, Laub F, Aldabe R, Zhang W, Ramirez F, Yoshida T and Terada M: Cloning the cDNA for a new human zinc finger protein defines a group of closely related Krüppel-like transcription factors. J Biol Chem 273: 28229-28237, 1998.
21. James-Zorn C, Ponferrada VG, Jarabek CJ, Burns KA, Segerdell EJ, Lee J, Snyder K, Bhattacharyya B, Karpinka JB, Fortriede J, *et al*: Xenbase: Expansion and updates of the Xenopus model organism database. Nucleic Acids Res 41: D865-D870, 2013.
22. Zhang Z, Wang H, Sun Y, Li H and Wang N: Klf7 modulates the differentiation and proliferation of chicken preadipocyte. Acta Biochim Biophys Sin (Shanghai) 45: 280-288, 2013.
23. Livak KJ and Schmittgen TD: Analysis of relative gene expression data using real-time quantitative PCR and the 2(-Delta Delta C(T)) Method. Methods 25: 402-408, 2001.
24. Tang D, Huang Y, Liu W and Zhang X: Up-regulation of microRNA-210 is associated with spermatogenesis by targeting IGF2 in male infertility. Med Sci Monit 22: 2905-2910, 2016.
25. Kelly TJ, Souza AL, Clish CB and Puigserver P: A hypoxia-induced positive feedback loop promotes hypoxia-inducible factor 1alpha stability through miR-210 suppression of glycerol-3-phosphate dehydrogenase 1-like. Mol Cell Biol 31: 2696-2706, 2011.
26. Feng Y, Zhu M, Dangelmajer S, Lee YM, Wijesekera O, Castellanos CX, Denduluri A, Chaichana KL, Li Q, Zhang H, *et al*: Hypoxia-cultured human adipose-derived mesenchymal stem cells are non-oncogenic and have enhanced viability, motility, and tropism to brain cancer. Cell Death Dis 5: e1567, 2014.
27. Salama R, Masson N, Simpson P, Sciesielski LK, Sun M, Tian YM, Ratcliffe PJ and Mole DR: Heterogeneous effects of direct hypoxia pathway activation in kidney cancer. PLoS One 10: e0134645, 2015.
28. de Motta LL, Ledaki I, Purshouse K, Haider S, De Bastiani MA, Baban D, Morotti M, Steers G, Wigfield S, Bridges E, *et al*: The BET inhibitor JQ1 selectively impairs tumour response to hypoxia and downregulates CA9 and angiogenesis in triple negative breast cancer. Oncogene 36: 122-132, 2017.
29. Li R, Geng HH, Xiao J, Qin XT, Wang F, Xing JH, Xia YF, Mao Y, Liang JW and Ji XP: miR-7a/b attenuates post-myocardial infarction remodeling and protects H9c2 cardiomyoblast against hypoxia-induced apoptosis involving Sp1 and PARP-1. Sci Rep 6: 29082, 2016.
30. Taraseviciene-Stewart L, Kasahara Y, Alger L, Hirth P, Mc Mahon G, Waltenberger J, Voelkel NF and Tuder RM: Inhibition of the VEGF receptor 2 combined with chronic hypoxia causes cell death-dependent pulmonary endothelial cell proliferation and severe pulmonary hypertension. FASEB J 15: 427-438, 2001.
31. Ma YL, Zhang LX, Liu GL, Fan Y, Peng Y and Hou WG: N-Myc downstream-regulated gene 2 (Ndrg2) is involved in ischemia-hypoxia-induced astrocyte apoptosis: A novel target for stroke therapy. Mol Neurobiol 54: 3286-3299, 2017.
32. Zhang Q, Fan K, Wang P, Yu J, Liu R, Qi H, Sun H and Cao Y: Carvacrol induces the apoptosis of pulmonary artery smooth muscle cells under hypoxia. Eur J Pharmacol 770: 134-146, 2016.
33. Kalakech H, Tamareille S, Pons S, Godin-Ribuot D, Carmeliet P, Furber A, Martin V, Berdeaux A, Ghaleb B and Prunier F: Role of hypoxia inducible factor-1α in remote limb ischemic preconditioning. J Mol Cell Cardiol 65: 98-104, 2013.
34. Janke K, Brockmeier U, Kuhlmann K, Eisenacher M, Nolde J, Meyer HE, Mairbäurl H and Metzen E: Factor inhibiting HIF-1 (FIH-1) modulates protein interactions of apoptosis-stimulating p53 binding protein 2 (ASPP2). J Cell Sci 126: 2629-2640, 2013.
35. Huang X, Yang K, Zhang Y, Wang Q and Li Y: Quinolinic acid induces cell apoptosis in PC12 cells through HIF-1-dependent RTP801 activation. Metab Brain Dis 31: 435-444, 2016.
36. McCormick RI, Blick C, Ragoussis J, Schoedel J, Mole DR, Young AC, Selby PJ, Banks RE and Harris AL: miR-210 is a target of hypoxia-inducible factors 1 and 2 in renal cancer, regulates ISCU and correlates with good prognosis. Br J Cancer 108: 1133-1142, 2013.
37. Mutharasan RK, Nagpal V, Ichikawa Y and Ardehali H: microRNA-210 is upregulated in hypoxic cardiomyocytes through Akt- and p53-dependent pathways and exerts cytoprotective effects. Am J Physiol Heart Circ Physiol 301: H1519-H1530, 2011.
38. Kaczynski J, Cook T and Urrutia R: Sp1- and Krüppel-like transcription factors. Genome Biol 4: 206, 2003.
39. Laub F, Aldabe R, Friedrich V Jr, Ohnishi S, Yoshida T and Ramirez F: Developmental expression of mouse Krüppel-like transcription factor KLF7 suggests a potential role in neurogenesis. Dev Biol 233: 305-318, 2001.
40. Kawamura Y, Tanaka Y, Kawamori R and Maeda S: Overexpression of Kruppel-like factor 7 regulates adipocytokine gene expressions in human adipocytes and inhibits glucose-induced insulin secretion in pancreatic beta-cell line. Mol Endocrinol 20: 844-856, 2006.